Egypt. J. Geo. **Vol. 66,** pp: 181-200 (2022)

Egyptian Journal of Geology
https://egjg.journals.ekb.eg

The Impact of Seasonal Weather Changes on the Accumulated Sediments within Back-Reef Environment around Umm Al-Maradim island- Kuwait

Alham Jassim Al-langawi
The Authority of Applied Education and Training-Science Department, The State of Kuwait

This study is based on petrographic, geochemical and mechanical analysis of all collected samples from the intertidal zone around the southern Umm Al-Maradim Island in Kuwait. The objective is to interpret the impact of seasons conditions on coral buildups around the island. Petrographic study revealed that the intertidal area is a part of a back-reef environment which is composed of the accumulation of broken up coral debris, coralline algae, foraminifera, echinoderms particles, bivalves, and gastropods. Generally, most abundant grain sizes along the shores are coarse and very coarse sand size, indicating short distance of transport and high wave action. Short transportation distance and fast sedimentation resulted in the accumulation of poorly sorted and strongly coarse to coarse skewed sediments. Detailed study of the samples shows variations in grain size parameters as well as type of accumulated sediments between the different seasons and locations along the island, which is mainly related to the differences in wind intensity, changes in prevailing wind direction, and biological activities affecting the coral reefs. Geochemical study suggests an aragonitic and low-Mg calcite composition for the coral fragments, as well as, a pathetic relationship between all tested major elements within the collected sediments.

Keywords: Coral Reefs, Umm Al-Maradim Island, Back-reef environment, Seasonal Variations, Kuwait, Arabian Gulf .

Introduction

Kuwait is located on the northwestern end of Arabian Gulf, where the marine environment includes 9 islands, the largest are Bubiyan, Umm Al-Maradim, Failaka, Kubber and Warba, and the smallest are Qauh, Miskan, Auhah and Umm Al-Namel. All are located almost parallel to the shoreline of Kuwait mainland. Umm Al-Maradim is situated near the marine borderline with Saudi Arabia (Fig.1). It is nesting terrain for turtles, home to diverse types of migratory and residential birds, and surrounded by coral reefs. Northern tip of Umm Al-Maradim Island is located at 28°40′56.92″N and 48°39′6.09″E, and the south tip is located at 28°40′39.42″N and 48°39′6.07″E with a maximum length of 673.41 meters. The maximum length from west to east is 332 meters and it is between 28°40′48.26″N and 48°38′59.76″E at the western side, and 28°40′48.03″N and 48°39′12.22″E at the eastern side. Umm Al-Maradim has an area equal to 1.02 km^2, with maximum elevation of four meters above sea-level. Deep waters encircle the island, and it is located 30 km from mainland Kuwait. Umm Al-Maradim is blanketed by densely packed grass and inhabited by migratory birds and rabbits. The island is undeveloped besides the coast-defense station, a jetty, and massive coast defense marina at its southern tip. The intertidal area is confined varying from five to twenty-five meters.

Al-Ghadban (1994) presented the only detailed study on Umm Al-Maradim. He concluded that the morphological placing of the island is because of 2 incidences of relative sea-level change at some stage in happened in Pliocene-Pleistocene time. Kassler (1973) suggested that Arabian shelf profile is relatively uniform, but locally disrupted by salt dome rises,

*Corresponding author: ajharock2011@hotmail.com
Received: 25/11/2022; Accepted: 27/02/2023
DOI: 10.21608/EGJG.2023.176984.1030

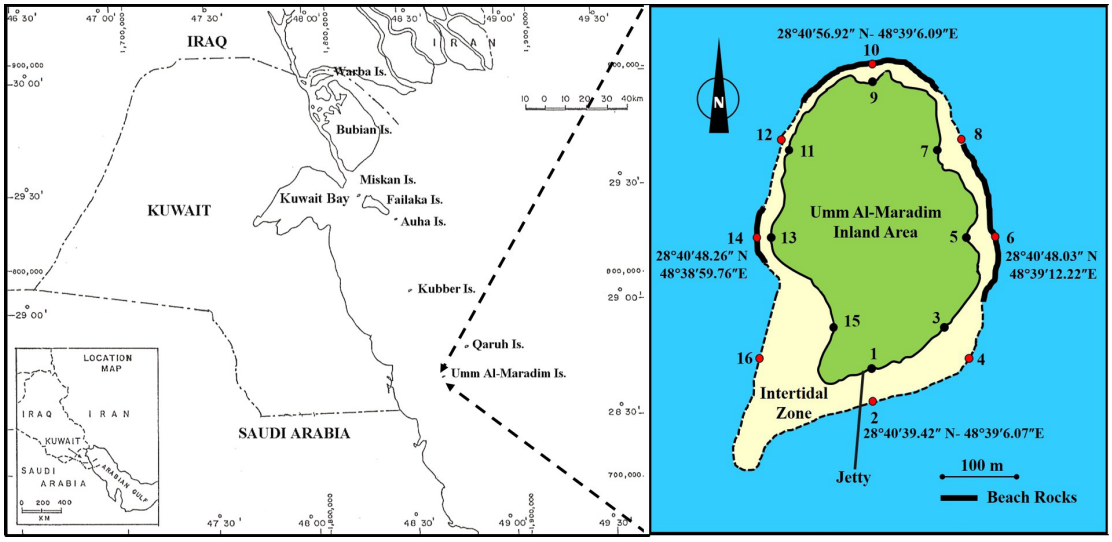

Fig. 1. Location map for Umm Al-Maradim Island showing sample locations.

coral covered sandbanks, and structurally controlled islands. Sellwood (1991) proposed fluctuations in sea-level during Pleistocene, which reached maximum low equals to –120 meters, occasionally uncovered the shelf ground and induced a sequence of river valleys and terraces. Thus, the existing Arabian Gulf underwater structure was a result of thousand years of subaerial exposure (Kassler, 1973). In general, calcareous beaches composed of numerous types of shells and coral fragments border Umm Al-Maradim. Al-Ghadban (1994) showed that the primary supply for the calcareous deposits is the indigenous constituents which resulted due to erosion on the coral build-ups, from many creatures dwelling along the corals, and from dust fallout due to storms. Highly consolidated gray and brown color carbonate rocks were found at the north, east and western, which are 20-40 cm thick and dipping approximately 13° towards the sea. The rock's composition is similar to the current intertidal sediments.

Umm Al-Maradim is a strategically important, important touristic area, and maintains a substantial fishery in Kuwait. Therefore, protecting the coral reefs around the island is hence essential. The current study contributes towards understanding of in what way does changing weather parameters affect coral reef, especially around Umm Al-Maradim, which is an essential first step to protect it. The abundance of marine life and various kinds of fish made the island a fishing and diving sites. Weather factors, including variable temperatures, wind direction and speed, rate of evaporation and its effect on water salinity, generally tend to vary between the seasons. Whether those factors are affecting the corals reefs or not is of great importance because it is linked to the aquatic food sources availability and productivity of the marine environment.

Methodology

Fieldwork and sampling

Ten fieldtrips were carried out to acquire samples during several months. The selected times for samplings were defined when learning the meteorological conditions, especially wind direction and speed, and temperature. Primary fieldtrips were throughout October which indicates the beginning of fall season. Then during January that marks the winter season in Kuwait. The last field trips were during June that marks the start of summer season. Eight geographic directions chosen for sampling are shown in (Fig. 1). Two samples were collected from every location: from low tide mark and high tide mark. A total of 48 samples were obtained from 3 different seasons. Samples were gathered from an area of about 900 cm^2 with a maximum depth of 2 cm.

Mechanical analysis of sediments

Mechanical analysis of the collected sediments conducted following sieving analysis constructed by Folk (1974). Folk and Ward (1957) formulae were used to calculate grain-size parameters including mean, median, skewness and sorting. There have been a few difficulties in calculating parameters for a few samples, for the ones having weight-retained percentage >5% within the first sieve. This difficulty resulted due to using first mesh = 4 mm, which retains grains of sizes more than or equal 4 mm, and the majority of retained grains are > 4 mm in size. Consequently, each sample

with the first weight percentage exceeds 5% was tested by hand to measure each grain by using a graticule thin section. The separated grain size is: > 32 mm, 32 - 16 mm, 16 - 8 mm, and 8 - 4 mm, indicative of -5 φ, -4 φ, -3φ, -2φ sizes. This technique helped in defining the parameters, which have provided false results for skewness and sorting.

Petrographic Study

Forty-eight samples were gathered and separated into 12 portions by using the sieve analysis technique. Therefore, a total of 576 samples were examined by the binocular stereomicroscope. Examination by polarizing microscope was carried out for selected samples. The abundance grading used was as follows: 1) Rare; ≤ 1%, 2) Common; ≤ 10%, 3) Abundant; ≥ 10%. Quantitative and qualitative analysis using the Scanning Electron Microscope (SEM) was carried out for chosen samples showing significant compositional variations or distinct features such as coral diversity and cement type. Solutions of potassium ferricyanide and alizarin Red-S were used to stain thinsections to assist in petrography. Mineralogical composition was obtained by using X-ray diffraction.

Geochemical Study

It is very important to state that, due to lack of time and restricted funds, chemical data is not completely and satisfactory presented. The author had to restrict chemical investigations on corals collected from high tide mark only. The size fraction equal to 0.5 mm was used in manually picking all coral fragments within the sediments. ICPms and X-ray fluorescence were used to measure the concentration of major and trace elements. The samples were examined in Earth and Environmental Science department- The University of Manchester.

Oceanography and Meteorology

Purser (1973a, b) indicated that the Arabian-Persian Gulf is a situated in a subtropical region and can be described an open shelf with a length equals to 1000 km and is 200-300 km wide. The depth of the Arabian Gulf varies between 35-100 m, and the west side slopes slightly toward the north. Sellwood (1991) postulated that the lower intertidal zone includes algal-grazing cerithids, pelletal lime, and burrowing crabs, whereas muddy sediments characterize the lower intertidal zones. Sellwood (1991) indicated that the mud is introduced in through storms and trapped by uninterrupted algal mats. He also indicated that more diverse fauna and flora are found living within channels cutting across the intertidal zones, and that coarse lags of shell debris and corals are densely coated with bryozoans and algae and affected by burrowing organisms.

In Kuwait the best-developed coral reefs are largely restricted around Umm Al-Maradim, Kubber and Qaruh Islands. Coral buildups in Kuwait exist in a tough ecosystem exposed to variable temperatures and contamination by oil. Currently the foremost challenges corals are facing are over- fishing, ships anchors, and human waste as indicated by Harrison et al., (1997). Dune movement, elevated temperature, mangroves, salinity, and sedimentation are the main conditions which elevate stressed reef-slope condition as suggested by Sheppard (1988). Two prime wind directions prevail during the year in Kuwait: "Kose" wind which blow from the southeast direction, and "Shamall" wind which blow from the northwest direction. Corals reefs around Umm Al-Maradim Island are affected by weather changes throughout the seasons. Temperature and water salinity similarly oscillate, averaging between 43.43% and 39.06%. Temperature gradually subsides and humidity increases after October which result in the shortage of nutrients as well as Oxygen, hence death of coral polyps through winter season. January mark the winter season in Kuwait and is characterized by the lowering of temperature, but temperature will be moderate from the end of February to end of March which will boost growth of algae. The monsoon season in Kuwait lasts through April and May, and it is characterized by thunder rainstorms and high wave action due to high wind velocity. High evaporation rates and partial separation of Arabian Gulf from Indian Ocean attributes to the abnormal marine salinities (Reading, 1991). Al-Ghadban, et al (1990) and Al-langawi (2013) determined that the eastern and western sides of Umm Al-Maradim are areas marked by Low and high wave strength, which is a result of the prevailing wind directions. Al-Ghadban, et al (1990) postulated that the main energy input coupled with wave efficiency confines to 20-30 meters and is attributed to the 'Shamal' winds.

Petrography

Composition of Sediment Samples

The petrographic study was based on preliminary examination by stereomicroscope of all sediment portions gathered after sieve analysis. Representative portions of each location were thinsectiond and examined by the polarizing microscope. Several samples were analyzed by the SEM quantitative and qualitative methods. The chosen samples include; bivalve particles covered by yellow micritic precipitate, hole and broken pieces of corals, gastropods, and foraminifera, and algal spores covered by coiled foraminifera and worm tubes.

The study of sediments by the stereomicroscope and polarizing microscope showed that all samples include the same bioclastic types but in various amounts. The

main bioclastic constituents include coral fragments, coralline algae, mollusks (especially gastropods and bivalves), and echinoderms fragments (Tables 1-3). Whereas minor bioclastic constituents consist of bryozoans, foraminifera, ostracods, worm tubes, oolitic grains, pellets, sponge spicules, and intraclasts. Coral fragments are the dominant bioclast exist in numerous types and sizes, and are affected by grain micritization and burrowing. Carbonate mud, botryoidal and prismatic crystal mesh of aragonite were found filling the intragranular porosity of the coarse coral fragments. It is found that shell fragments of both gastropods and bivalves are affected by grain micritization, while their original structure and composition is preserved. The intragranular pore spaces of gastropods are occluded by needle-shaped aragonite crystals or micrite cements. Different kinds of echinoderms are found and rarely affected by micritization. Usually, sediments collected in January show a higher degree of micrite cementation and grain micritization than bioclasts gathered throughout October and June. It is also noted that burrowing of shell fragments such as coralline algae, mollusks, and coral fragments was more intense than other bioclasts. Different species of coiled foraminifera exist within the intertidal sediments. These include; several types of Globigerinoides sp. (d'Orbigny) which is planktonic deep marine foraminifera, Trisegmentina sp., Spirllina Limbate Brady sp. and Alveollin sp. which are marine benthic foraminifera, and Ovate tests of Nummulites sp. and Elphidium sp. which dwell in shallow marine wave-influenced environment.

Scanning Electron Microscope investigation of the algal particles that are covered by coiled foraminifera revealed that the coiled foraminifera and worm tubes are cemented onto algae fragments by organic filamentlike matter, and longitudinal calcium carbonate (aragonite) crystals fill the void spaces of these foraminifera and worm tubes (Fig. 2). The aragonite crystals are thicker at the center and flattened at the edges. The aragonite cement and the filamentlike matter may possibly be of microbial origin. Brachiopod shell fragments are rare, and ostracods exist but in very low concentrations. SEM study revealed that radiolarian, foraminifera, bryozoans, and coccoliths fill intragranular spaces of some coarse bioclasts. SEM investigations also revealed extensive burrowing of bioclasts, especially bivalves, and the precipitation of micrite in these pores

The non-bioclastic fragments mainly include intraclasts of different sizes, as well as a few peloids and ooids. The most dominant particles are the intraclasts and appear to be developed after binding grains of corals, shell fragments, and ooids by either micritic or clear crystals. Ooids are rare and exist as fine superficial grains. Pellets (peloids) are even rare and appear as elliptical micritic grains. Non-carbonate (clastic) components do exist at all locations. The most abundant clastic component is quartz, which is mainly of metamorphic, igneous, and aeolian origins. Quartz grains are generally rounded - well rounded, and a few are angular. Most quartz grains are of aeolian origin, especially those of sizes < 0.5 mm. Other clastic constituents include oxidized iron particles, heavy minerals (iron oxides and mafic minerals), metallic particles, feldspars, and rock fragments, where the most dominant are the oxidized iron particles. Sediments accumulated throughout June and October show high percentage of prismatic and cubic crystals of sizes < 0.063 mm, which are mainly occurring as free crystals (Tables 1 and 2). Petrographic study indicated that these crystals are composed of halite, Mg-calcite, and gypsum. The main pollutant is believed to be oil which contaminated all accumulated sediments during the different seasons. The primary source of oil is oil tankers, that pass the Umm Al-Maradim while heading towards the oil port of Ahmadi. Petrographic study showed that oil contamination is in the form of free spherical tar grains, clogging porosity of bioclasts, and forming tar cover around some fragments.

Intragranular porosity within bioclasts is cemented by high-Mg prismatic calcite crystals, and microcrystalline, needle form isopachous, and botryoidal aragonite cement (Fig. 3). Sediments accumulated throughout June and October are more particularly affected by cementation than grains accumulated throughout January. Furthermore, cubic form halite cement is higher during June and October than the month of January (Tables 1-3). Additionally, a yellowish orange and yellow microcrystalline cement coats several particles, and white color micritic is the binding matter for few intraclasts. Brown color filamentlike matter was also observed cementing bioclasts to algal fragments. Scanning Electron Microscope investigation showed that the yellow micritic cementing crystals is composed of gypsum and halite. Moreover, the SEM study indicated that cementing crystals on particles are composed of aragonite, halite, and Mg-calcite of a variety of forms and dimensions (Fig. 2 and 4).

Grain Size Technique

Histograms and Their Indications

Particle size technique is a tool conducted to highlight the effectiveness of meteorological factors, for example wind direction and wind speed, hence the effect on sustainability of any fauna and flora communities living within marine environments. Each sample will give indication of the proportions of particles sizes after conducting the experiment, which

TABLE 1. Sample description of October sediments by stereomicroscope. Whole and broken = (w&b).

Sieve (mm)	High tide Mark	Low tide Mark
32	No sediments	Composed of coral fragments, bivalve, and intraclasts. Affected by micritization, burrowing, and oil contamination
16	Composed of bivalves and coral fragments	Composed of diverse types of corals, (w&b) bivalves, intraclasts (cemented by micrite). Affected by micritization, burrowing, and oil contamination
8	Composed of coral fragments and (w&b) bivalve shells, few affected by micritization and burrowing	Composed of diverse types of corals, (w&b) mollusks, intraclasts. Affected by micritization, burrowing, and oil contamination
4	Composed of bivalves and coral fragments, some are micritized	Composed of more diverse types of corals, (w&b) mollusks, intraclasts. Affected by micritization, burrowing, oil contamination, and cementation by prismatic crystals.
2	Composed of corals, (w & b) mollusks, and intraclasts. Affected by micritization and oil contamination. There exist few cubic cementing crystals	Composed of more diverse types of corals, (w&b) mollusks, echinoderms spines, rusty iron particles, intraclasts (cemented by prismatic and cubic crystals). Affected by cementation by needle-shape cement, and oil contamination.
1	Composed of corals, (w & b) mollusks, echinoderm spines, sand, and intraclasts. Few bioclasts are affected by grain micritization and oil contamination. There exist few cubic cementing crystals on grain surfaces and prismatic cementing crystals within porosity	Composed of corals, mollusks, echinoid spines, oolitic grains, worm tubes, rusty iron particles, intraclasts. Affected by micritization, oil contamination, and cementation by cubic and prismatic crystals.
0.5	Composed of diverse types of corals, (w&b) mollusks shells, echinoid spines and plates, oolitic grains, pellets, sand, bryozoan, rusty iron particles, and intraclasts. Affected by oil contamination, cementation by cubic and prismatic crystals, and grain micritization	Composed of corals, (w&b) mollusks, echinoderm spines, oolitic grains, sand, bryozoans, intraclasts. Affected by micritization, oil contamination, and cementation by cubic and needle shape crystals.
0.25	Composed of mollusks, corals, echinoderms plates and spines, (w&b) forams, oolitic grains, pellets, high amount of sand, bryozoans, intraclasts, rusty iron particles. Affected by grain micritization and cementation by prismatic and cubic crystals, and oil contamination	Composed of mollusks, corals, echinoderms plates and spines, (w&b) forams, oolitic grains, bryozoans, (w&b) ostracods, and intraclasts. Affected by micritization, oil contamination, and cementation by cubic and needle shape crystals. Occurrence of free cubic crystals
0.125	Composed of mollusks, corals, echinoderms plates and spines, (w&b) forams, oolitic grains, pellets, sand, bryozoans, intraclasts, ostracods, worm tubes. Some are micritized. Affected by cementation by prismatic and cubic crystals, and oil contamination	Composed of mollusks, corals, echinoid plates and spines, (w&b) forams, oolitic grains, (w&b) ostracods, bryozoan, rusty particles, sand, and intraclasts. Affected by micritization, oil contamination, cementation by cubic and needle shape crystals. Occurrence of free cubic crystals
0.063	Composed of mollusks, corals, echinoid plates, forams, sponge spicules, ostracods, oolite, sand, and heavy minerals. Affected by micritization, cementation by prismatic and cubic crystals, and oil contamination. There exist free prismatic and cubic crystals.	Composed of corals, mollusks, forams, ostracods, echinoid spines, sand, heavy minerals, intraclasts, and sponge spicules. Affected by micritization, oil contamination, and cementation by needle shape crystals.
0.036	Composed of (w&b) forams, corals, mollusks, heavy minerals, and sand. Contains high quantity of free prismatic and cubic minerals	Composed of forams, corals, sponge spicules, echinoderms, ostracods, heavy minerals, and sand. Free prismatic crystals
Pan	No sediments	No sediments

TABLE 2. Sample description of June sediments by stereomicroscope. Whole and broken = (w&b).

Sieve (mm)	High tide Mark	Low tide Mark
32	Composed of bivalves and coral fragments	No sediments
16	Composed of diverse types of coral fragments and (w&b) bivalve shells, affected by oil contamination	Composed of bivalves and coral fragments, few cemented grains on surface of bioclasts. Affected by oil contamination
8	Composed of coral fragments, (w&b) mollusks shells, and intraclasts, and affected by oil contamination	Composed of coral fragments, (w&b) mollusks shells, few cemented grains on surface of bioclasts. Affected by grain micritization and oil contamination
4	Composed of diverse types of corals, (w&b) mollusks shells, and intraclasts, and affected by oil contamination and micritization	Composed of diverse types of corals, (w&b) mollusks shells, and intraclasts (few cemented by filamentous substance). Affected by grain micritization, few cemented grains on surface of bioclasts, and oil contamination
2	Composed of diverse types of corals, (w&b) mollusks shells, intraclasts (few cemented by fibrous translucent to transparent substance). Affected by micritization and oil contamination	Composed of diverse types of corals, (w&b) mollusks shells, echinoid spines, intraclasts, sand. Affected by rare grain micritization, few cemented grains on surface of bioclasts, cubic crystals, and oil contamination
1	Composed of diverse types of corals, (w&b) mollusks shells, echinoderms spines, oolitic grains, sand, and intraclasts (few cemented by micrite and fibrous translucent to transparent substance). There exist a few cubic cementing crystals and fibrous needle shaped cement crystals on grain surfaces. There exists contamination by oil and tar particles	Composed of corals, (w&b) mollusks shells, bryozoans, echinoid spines, sand, intraclasts. Affected by cementation by cubic crystals, and oil contamination
0.5	Composed of diverse types of corals, (w&b) mollusks shells, echinoid spines and plates, oolitic grains, pellets, sand, bryozoan, forams, and intraclasts (some cementation by cubic halite and micrite). Affected by oil contamination and particles	Composed of diverse types of corals, (w&b) mollusks, echinoids, forams, bryozoans, sand, annelid tubes, oolitic grains, pellets, intraclasts (few joined by white micrite and crystalline cement). Affected by cementation by cubic crystals, and oil contamination
0.25	Composed of diverse types of corals, (w&b) mollusks shells, echinoid spines and plates, oolitic grains, pellets, sand, bryozoan, (w&b) diverse types of forams, ostracods, intraclasts. Affected by cubic and prismatic cementing crystals on grain surfaces, and oil contamination plus particles.	Composed of diverse types of corals, (w&b) mollusks shells, echinoid spines and plates, high number of oolitic grains, pellets, sand, bryozoan, (w&b) diverse types of forams, ostracods, worm tubes, intraclasts. Affected by cementation by prismatic and cubic crystals, and oil contamination. Free prismatic and cubic crystals exist
0.125	Composed of (w & b) mollusks, corals, echinoderm spines, diverse types of forams, ostracods, worm tubes, bryozoans, fish bones, oolitic grains, pellets, sand, and intraclasts. Affected by cubic and prismatic cementing crystals on grain surfaces, and oil contamination plus particles	Composed of (w & b) mollusks, corals, echinoid spines, a high number of diverse types of forams, bryozoans, worm tubes, ostracods, sand, and high number of ooids. Affected by cubic and prismatic cementing crystals on grain surfaces, and oil contamination plus particles
0.063	Composed of mollusks, corals, echinoderm spines, (w&b) forams, oolitic grains, high number of sands, ostracods, fish bones, bryozoans, worm tubes, metallic particles. Affected by cubic and prismatic cementing crystals on grain surfaces, and oil contamination plus particles	Composed of (w & b) mollusks, corals, echinoderm spines, forams, bryozoans, oolitic grains, sand, heavy minerals, metallic particles. Affected by prismatic cementing crystals on grain surfaces. Free prismatic and cubic crystals exist
0.036	Composed of few bioclastic grains and sand, with high amount of free prismatic and cubic crystals	No sediments
Pan	No sediments	No sediments

TABLE 3. Sample description of January sediments by stereomicroscope. Whole and broken = (w&b).

Sieve (mm)	High tide Mark	Low tide Mark
32	Composed of coral fragments and bivalve shells, few affected by burrowing, but highly micritized	Composed of coral fragments, affected by burrowing, micritization, and oil contamination
16	Composed of fragments of bivalve, corals, gastropods and intraclasts. Few affected by micritization, burrowing, and oil contamination	Composed of diverse types of corals, (w&b) mollusks. Affected by micritization, burrowing, oil contamination, and cemented of intragranular porosity
8	Composed of diverse types of coral fragments, (w&b) mollusk shells, and intraclasts (few are cemented by micrite). And affected by micritization, burrowing, and oil contamination	Composed of diverse types of coral fragments, (w&b) mollusk, and intraclasts. Affected by micritization, burrowing, oil contamination, and cemented of intragranular porosity by clear and micritic crystals
4	Composed of diverse types of coral fragments, (w&b) mollusk shells, and intraclasts. And affected by micritization, burrowing, and oil contamination	Composed of coral fragments, diverse (w&b) mollusks, intraclasts. Affected by micritization, burrowing, oil contamination, and cementation by prismatic and micritic crystals of grain surfaces
2	Composed of diverse types of coral fragments and (w&b) mollusk shells, annelid tubes, intraclasts. Affected by pronounced micritization, burrowing, oil contamination, and cementation of porosity. There exist some benthic forams cemented to algal spores	Composed of diverse types of coral fragments and (w&b) mollusk shells, intraclasts (cemented by micrite and filamentous substance), rusty particles, wood fragments. Affected by micritization, burrowing, oil contamination, and cementation of porosity by cubic and prismatic crystals
1	Composed of diverse types of coral fragments and (w&b) mollusk shells, oolitic grains, sand, echinoderms spines, and intraclasts. Affected by micritization, burrowing, oil contamination. There exist some benthic forams cemented to algal spores, and precipitation of yellow substance on some particles	Composed of diverse types of coral fragments and (w&b) mollusk shells, echinoid spines, reworked glass, sand, intraclasts (some cemented by prismatic & cubic cement). Affected by micritization, burrowing, oil contamination, and cementation by prismatic, cubic, and yellow micritic substance
0.5	Composed of corals, (w&b) mollusks, echinoderms, (b) forams, oolitic grains, annelid tubes, reworked glass, sand, intraclasts (few cemented by micrite). Bioclasts are highly micritized and cemented by a few cubic crystals and fine yellow substances. Contamination by oil	Composed of corals, (w&b) mollusks, echinoderms, (b) forams, oolitic grains, annelid tubes, reworked glass, sand, intraclasts (few cemented by crystalline cement). Affected by moderate micritization, burrowing, oil contamination, and cementation by prismatic, cubic, and yellow and reddish-brown micritic substance
0.25	Composed of corals, (w&b) mollusks, echinoderms, forams (w&b), sand, glass particles, pellets, rust grains, oolitic grains, annelid tubes, bryozoans, intraclasts. Affected by great micritization, burrowing, precipitation of yellowish-brown substance and cubic crystals, and contamination by oil	Composed of corals, (w&b) mollusks, echinoderms, diverse types of (w&b) forams, bryozoans, oolitic grains, ostracods, pellets, reworked glass, sand, and intraclasts (some cemented by prismatic & cubic cement). Affected by micritization, burrowing, oil contamination, and cementation by prismatic, cubic, and yellow and reddish-brown micritic substance. Occurrence of free cubic crystals
0.125	Composed of corals, (w&b) mollusks, echinoderms, (w&b) forams, sand, glass particles, pellets, rust grains, oolitic grains, ostracods. Some cementations by prismatic and cubic crystals, and fine yellowish substance on grain surfaces, and oil contamination plus particles	Composed of corals, (w&b) mollusks, echinoderms, (w&b) forams, sand grains, glass particles, peloids, metallic particles, oolitic grains, ostracods, bryozoans, and intraclasts (few cemented by clear crystals. metallic particles. Affected by oil contamination, and cementation by prismatic, cubic, and yellow micritic substance
0.063	Composed of mollusks, corals, echinoids, forams, bryozoans, annelid shells, sponge spicules, sand, reworked glass, oolitic grains, metallic particles. Affected by prismatic and cubic crystals, and oil contamination. There exist free prismatic and cubic crystals	Composed of mollusks, corals, echinoids, diverse forams, bryozoans, ostracods, annelid shells, oolitic grains, metallic particles, sand. Affected by oil contamination, and existence of free prismatic and cubic crystals
0.032	Mainly mollusks, corals, echinoid spines, forams, bryozoans, sand, oolitic and metallic particles. Contain rare free cubic and prismatic crystals, and oil contamination plus particles	Composed of coral fragments, mollusks, bryozoans, forams, sponge spicules, metallic and tar particles, sand, and free cubic and prismatic crystals
Pan	No sediments	No sediments

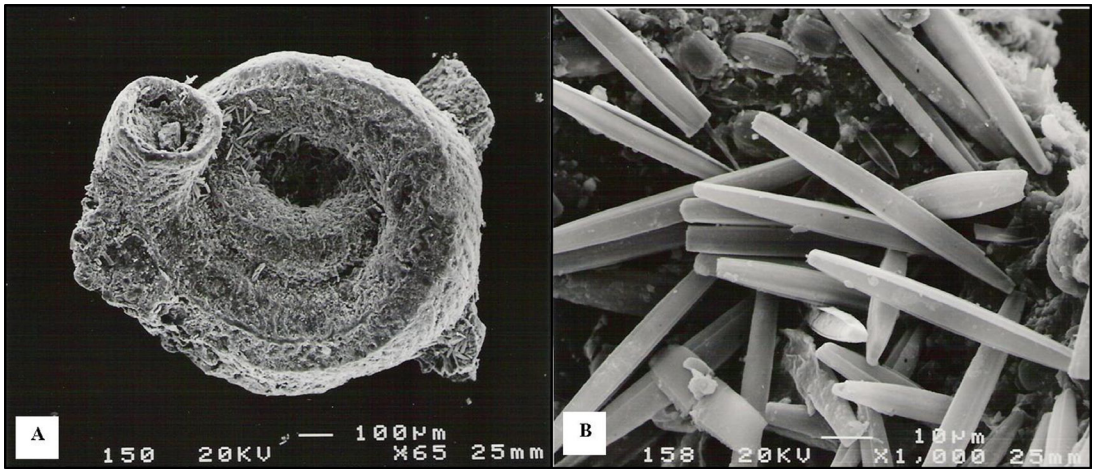

Fig. 2. SEM Backscattered photographs showing (A) One worm tube cemented by longitudinal aragonite crystals, B) Close up view of the Aragonite crystals mesh.

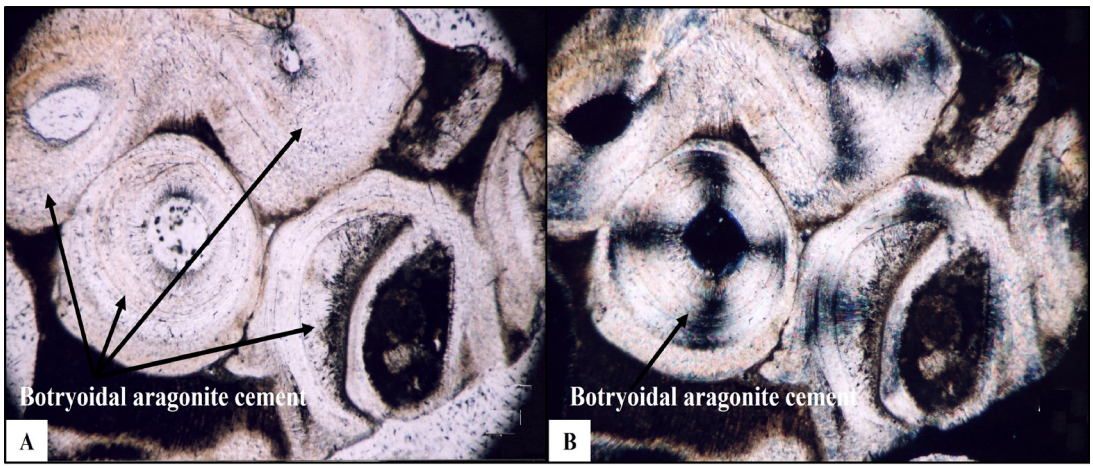

Fig. 3. Photographs displaying intragranular porosity cementation of gastropod fragment by botryoidal aragonite crystals. A) Under ppl, B) Under xpl. Magnification= 10x.

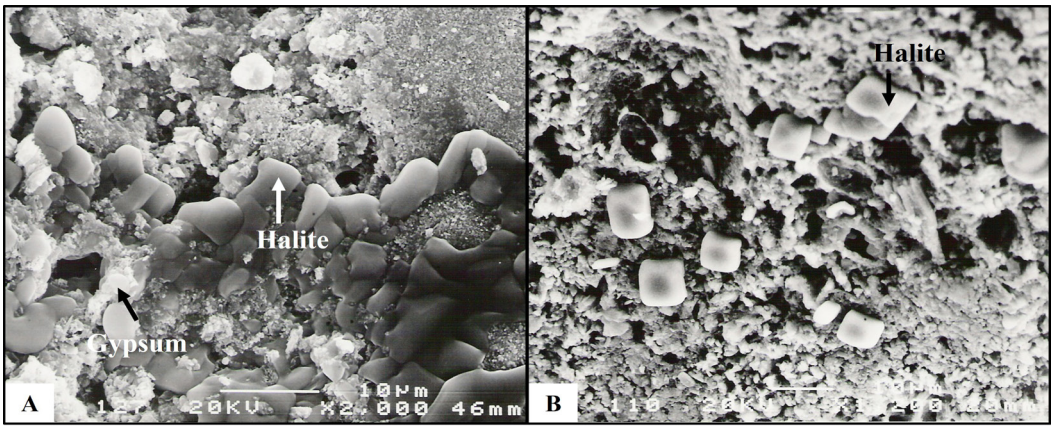

Fig. 4. Backscattered images showing (A) Cementing crystals of Halite and Gypsum, B) Cementing crystals of Halite on collected sediments.

should be presented as histograms and frequency curves. Figure (5) explain the grain size dispersal of intertidal zone sediments taken from Umm Al-Maradim in a form of histograms. Figure (5-A) shows that sediments gathered throughout October from high tide mark are mostly well to moderately sorted with a grain size distribution varies between very coarse sand to fine sand size. There exist one sample which is collected from the southeast (M5) is poorly sorted, where the grain sizes range from fine sand to pebble size (Fig. 5-A and B). Sediments gathered from low tide mark are considerably variable in sizes. The constructed histogram shows no specific size groups and that some samples include mainly coarse fragments and others composed of fine grain sizes (Fig. 5-B). Figure (5-C and D) includes histograms explaining the distribution of particle sizes within intertidal environment throughout January. Figure (5-C) indicates that most accumulated sediments at high tide points gather at very coarse size to fine sand sizes, and only some have particle distribution ranging from pebble size to fine sand size. Grain size distribution suggests that high tide deposits are generally well to moderately sorted and the minority of samples are poorly sorted. Even though the majority of low tide grains gather around very coarse sand size to fine sand size, it appears that some samples fall within pebble to granule size categories (Figure 5-D). Hence suggesting that most accumulated sediments at low tide mark are poorly sorted. Figure (5-E and F) includes histograms explaining the grain size dispersion of intertidal sediments accumulated in the month of June. Both histograms indicate that both low tide and high tide deposits are equally similar as grain sizes gather at very coarse sand size to fine sand size, and only some specimens have dispersion range from pebble size to fine sand size. Grain size distribution suggests that grains accumulated at both low tide and high tide are mostly well to moderately sorted and only some are poorly sorted.

Histograms shown in Figure 5 for all samples collected in October demonstration that entire high tide deposits are well - moderately sorted, whereas grains collected from low tide mark are poorly sorted, excluding samples number M2, M6, and M14 which are classified as well- moderately sorted. Histograms of all samples collected in June show that almost all high tide samples are well to moderately sorted, apart from samples M1, M3, and M7 which are poorly sorted. Samples collected from low tide mark are poorly sorted, apart from samples M2 (southwest) and M16 (west), which are well sorted. Histograms of all samples collected in January show that most samples collected from high tide mark are poorly sorted, except for samples M9, M13, and M15 which are well sorted. Almost all samples collected from low tide mark are poorly sorted, except for sample M14 which is well to moderately sorted.

Grain Size Parameters and Their Indications

Normally it is impossible to gain all knowledge on sorting and skewness from histograms i.e., particle size distribution graphs as well as frequency curves.

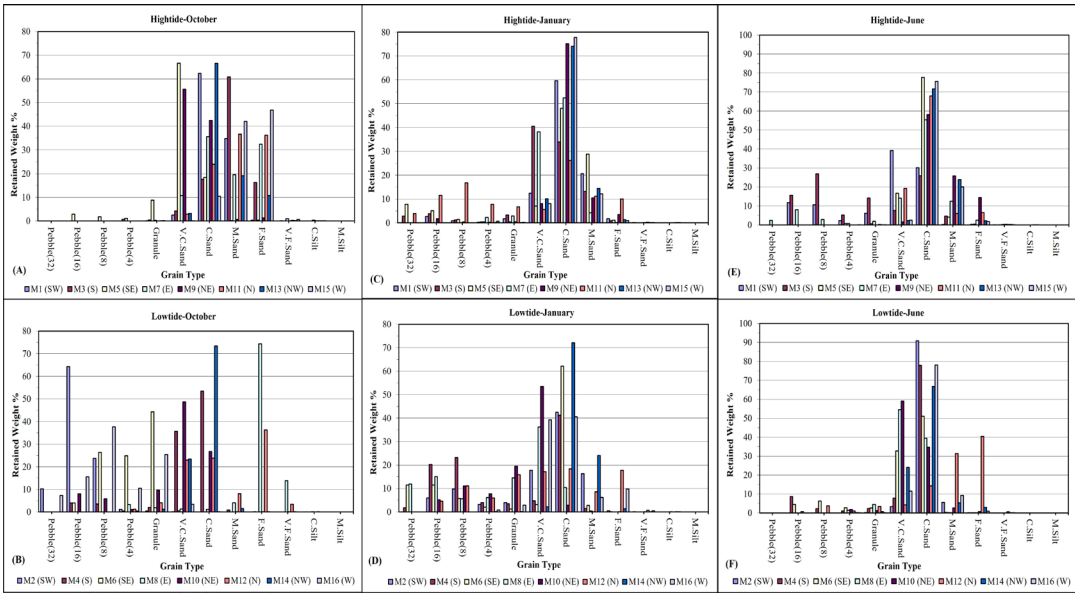

Fig. 5. Particle size dispersion histograms for accumulated sediments within the intertidal zone around Umm al-Maradim Island-Kuwait.

Therefore, cumulative graphs should be drawn out of the sizes gained after sieving technique and then calculating the different parameters to establish better results especially regarding skewness and sorting of accumulated sediments. Table (4) records the complete results and equivalent indicators which are acquired from the frequency curves. Table (5) listing the complete results and equivalent indicators with the aid of using Folk and Ward (1957) formulae using cumulative curves. The statistics for the entire number of samples collected during the seasons indicate that Mode results cluster at 5 grain size groups (Fig. 6). Both Cumulative curves and histograms demonstrate that 60.42% of entire number of samples the Mode peaks correspond to coarse sand size category, the Mode of 18.75% of samples falls at very coarse sand size category, the Mode of 8.33% of the samples falls at granule size category, the mode for 8.33% of samples falls at fine sand size category, and the Mode for 4.17% of samples falls at medium sand size category. Statistics suggest that the size of most of the grains is coarse sand size. As for Sorting, the data suggest that 2.08% of all samples show a very well sorting nature, 50% of samples show a well sorting nature, and 47.92% of all samples show poorly sorting (Table 4 & Fig. 7-A). On the other hand, data regarding Skewness gained from frequency curves indicated that 45.83% of the entire number of gathered samples are coarse skewed, skewness of 35.42% of samples is near symmetrical, 4.17% are symmetrical, and 14.58% of samples are fine skewed (Table 4, and Fig. 7-C).

Statistical data indicate generally that the accumulated sediments include the following Median terms: 52.08% are falls at coarse sand category, 24.99% falls at very coarse sand category, 12.5% falls at granules category, 8.33% falls at medium sand size category, and 2.08% falls at coarse sand size category (Table 5, and Fig. 6-D). This implies that half of particles comprising the samples are larger than coarse sand size and half are smaller than coarse sand size within 52.8% of all gathered samples, and hence forward for the rest of the samples. Parameters statistics also show that the most frequent Mean grain sizes in 47.92% of samples is coarse sand size, 22.92% of samples is very coarse sand size, 18.75% of samples are of granules size, 14.58% of samples are of fine sand size, and 8.33% of samples are medium sand size (Table 5 & Fig. 6-D). The data also suggest that 41.67% of collected samples are poorly sorted, 22.92% are moderately-well sorted, 18.75% of the samples are well sorted, 14.58% are moderately sorted, and 2.083% are very well sorted (Table 5, and Fig. 7-B). Parameters statistics regarding Skewness show that 2.08% of all the samples are symmetrical, 8.33% are fine skewed, 33.33% are strongly fine skewed, and 54.17% are strongly coarse skewed (Table 5, and Fig. 7-D).

Geochemical Results

The purpose of chemical analysis is to identify any chemical variations in the composition of the accumulated coral particles along the shores of Umm Al-Maradim Island and to explain the link with weather changes throughout the seasons. This section describes the fluctuation of major and trace elements concentration in the coral fragments obtained throughout the different seasons. Only coral fragments collected from high tide mark and of size equals to 0.5 mm were used in this investigation. The concentrations of major elements of Ca, Mg, Na, Al, Si, K, Fe, and Sr, and trace elements of Cu, Co, Cr, Pb, and Zn will be presented in this section.

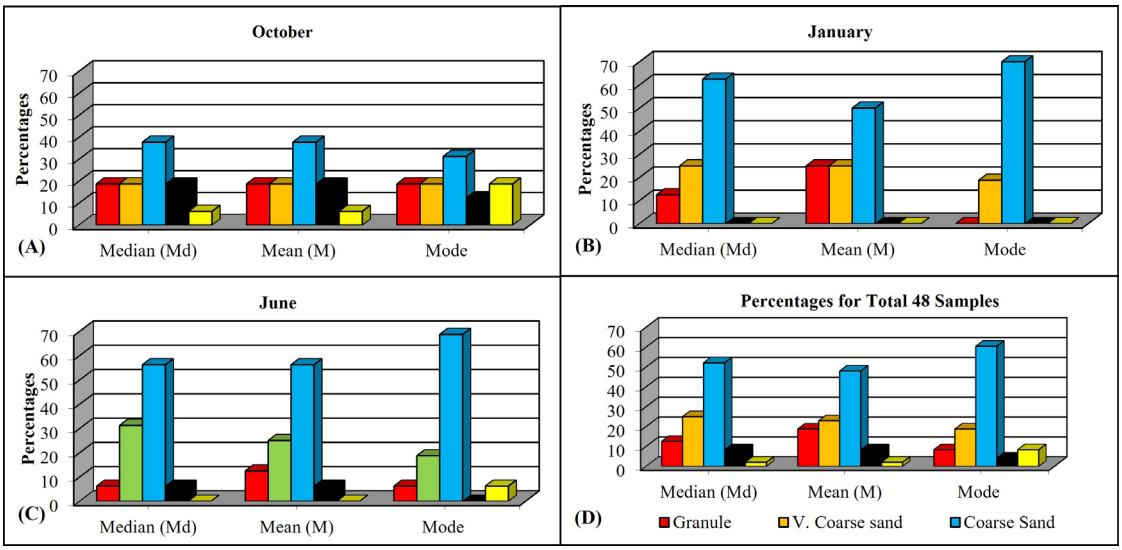

Fig. 6. Histograms showing percentage of grain size parameters.

TABLE 4. Parameters results according to Frequency Distribution Curves. Odd numbers are for high tide samples even numbers are for low tide samples.

Sample No.	Direction	October			January			June		
		Mode (mm)	Sorting (σ)	Skewness	Mode (mm)	Sorting (σ)	Skewness	Mode (mm)	Sorting (σ)	Skewness
M1	SW	0.5 Coarse Sand	Well Sorted	Near symmetrical	0.5 Coarse Sand	Well Sorted	Coarse Skewed	1 V. Coarse Sand	Poorly Sorted	Coarse Skewed
M2	SW	16 Granule	Well Sorted	Fine Skewed	0.5 Coarse Sand	Poorly Sorted	Coarse Skewed	0.5 Coarse Sand	V. Well Sorted	Symmetrical
M3	S	0.25 Medium Sand	Well Sorted	Near symmetrical	1 V. Coarse Sand	Poorly Sorted	Coarse Skewed	8 Granule	Poorly Sorted	Fine Skewed
M4	S	0.5 Coarse Sand	Poorly Sorted	Coarse Skewed	0.5 Coarse Sand	Poorly Sorted	Coarse Skewed	0.5 Coarse Sand	Poorly Sorted	Coarse Skewed
M5	SE	1 V. Coarse Sand	Well Sorted	Coarse Skewed	0.5 Coarse Sand	Poorly Sorted	Coarse Skewed	0.5 Coarse Sand	Well Sorted	Near symmetrical
M6	SE	4 Granule	Poorly Sorted	Coarse Skewed	0.5 Coarse Sand	Poorly Sorted	Coarse Skewed	0.5 Coarse Sand	Poorly Sorted	Coarse Skewed
M7	E	0.5 Coarse Sand	Poorly Sorted	Coarse Skewed	0.5 Coarse Sand	Well Sorted	Near symmetrical	0.5 Coarse Sand	Poorly Sorted	Coarse Skewed
M8	E	0.125 Fine Sand	Well Sorted	Coarse Skewed	1 V. Coarse Sand	Poorly Sorted	Coarse Skewed	1 V. Coarse Sand	Well Sorted	Near symmetrical
M9	NE	1 V. Coarse Sand	Well Sorted	Fine Skewed	0.5 Coarse Sand	Well Sorted	Near symmetrical	0.5 Coarse Sand	Well Sorted	Near symmetrical
M10	NE	1 V. Coarse Sand	Poorly Sorted	Coarse Skewed	1 V. Coarse Sand	Poorly Sorted	Coarse Skewed	1 V. Coarse Sand	Well Sorted	Near symmetrical
M11	N	0.25 Medium Sand	Well Sorted	Near symmetrical	0.5 Coarse Sand	Poorly Sorted	Coarse Skewed	0.5 Coarse Sand	Poorly Sorted	Fine Skewed
M12	N	0.125 Fine Sand	Poorly Sorted	Coarse Skewed	0.5 Coarse Sand	Poorly Sorted	Coarse Skewed	0.125 Fine Sand	Poorly Sorted	Coarse Skewed
M13	NW	0.5 Coarse Sand	Well Sorted	Fine Skewed	0.5 Coarse Sand	Well Sorted	Near symmetrical	0.5 Coarse Sand	Well Sorted	Near symmetrical
M14	NW	0.5 Coarse Sand	Well Sorted	Near symmetrical	0.5 Coarse Sand	Well Sorted	Near symmetrical	0.5 Coarse Sand	Well Sorted	Near symmetrical
M15	W	0.125 Fine Sand	Well Sorted	Near symmetrical	0.5 Coarse Sand	Well Sorted	Near symmetrical	0.5 Coarse Sand	Well Sorted	Near symmetrical
M16	W	8 Granule	Poorly Sorted	Fine Skewed	0.5 Coarse Sand	Poorly Sorted	Fine Skewed	0.5 Coarse Sand	Well Sorted	Symmetrical

Table 6 lists $CaCO_3$ and $MgCO_3$ Mole% for all the corals at high tide and show that $CaCO_3$ range between 93.23-98.37 Mole% ±1.06, and $MgCO_3$ range between 1.63-6.77 Mole% ±1.06 for all collected coral fragments. These results imply that all the corals are composed of low-Mg calcite or Aragonite. Figure 8 indicate that coral fragments from all the seasons has nearly the same concentrations of $CaCO_3$ Mole %. The results are comparable, except for the sample collected from the SW during October which show a slightly decreasing $CaCO_3$ Mole% compared to other seasons (Fig. 8-A). The lowest $CaCO_3$ Mole% and highest $MgCO_3$ Mole% concentration is present in the samples collected from during June, especially at the south direction (Fig. 8-C).

The other major elements are arranged in order of concentration values as follows; Al, Na, Si, Sr, Fe, and the least is K (Table 6). Concentration values of Aluminum in coral fragments from all the seasons range between 139-27300 ppm ±5442, sodium concentration in coral fragments from all the seasons range between 3149-16300 ppm ±3042, silicon concentration in coral fragments from all the seasons range between 3510-13000 ppm ±2258, strontium in coral fragments from all the seasons concentration range between 5890-7863 ppm ±598, iron in coral fragments from all the seasons concentration range between 245-1080 ppm ±176, and potassium in coral fragments from all the seasons concentration range between 147-1040 ppm ±177. Figure 9 is line graph showing the distribution of all major elements according to sample location and in the different seasons. The staked graphs (Fig. 9- B, D and F) clearly show a pathetic relationship between all elements and in all geographic locations, except for the southwest location in corals collected during October (Fig. 9–A), where concentration levels relatively drop than January and June. Generally, the highest concentration levels of major elements is in coral fragments collected from the S, E, N, and W directions throughout all the seasons, whereas the lowest concentration levels are in coral fragments collected from the SE, NE, and NW. Table 6 clearly show that all the highest concentrations data for N, K, Al, Fe, and Sr are obtained from coral fragments collected from the south of the island during the month of June, except for Sr data the highest concentration is within coral fragments collected from the NW in June.

Trace elements of Cr, Co, Cu, Zn, and Pb is presented in (Table 6), where it clearly shows that all of these elements are present in very low concentrations and that the majority of samples show Pb and Zn concentrations below the detection limits. Figure 10 is line graph showing the distribution of trace elements

TABLE 5. Parameters results according to grain-size analysis. Odd numbers are for high tide samples even numbers are for low tide samples.

Sample No.	Direction	October				January				January			
		Median (Md)	Mean (M)	Sorting (σ)	Skewness	Median (Md)	Mean (M)	Sorting (σ)	Skewness	Median (Md)	Mean (M)	Sorting (σ)	Skewness
M1	SW	Coarse Sand	Coarse Sand	Moderately Well	Strong Fine Skewed	Coarse Sand	Coarse Sand	Moderately Sorted	Strong Coarse Skewed	Very Coarse Sand	Granule	Poorly Sorted	Strong Coarse Skewed
M2	SW	Granule	Granule	Moderately Well	Strong Fine Skewed	Coarse Sand	Very Coarse Sand	Poorly Sorted	Strong Coarse Skewed	Coarse Sand	Coarse Sand	Very Well Sorted	Symmetrical
M3	S	Coarse Sand	Coarse Sand	Well Sorted	Strong Fine Skewed	Very Coarse Sand	Very Coarse Sand	Poorly Sorted	Strong Coarse Skewed	Granule	Granule	Poorly Sorted	Fine Skewed
M4	S	Coarse Sand	Coarse Sand	Poorly Sorted	Strong Coarse Skewed	Granule	Granule	Poorly Sorted	Strong Coarse Skewed	Coarse Sand	Coarse Sand	Poorly Sorted	Strong Coarse Skewed
M5	SE	Very Coarse Sand	Very Coarse Sand	Moderately sorted	Strong Coarse Skewed	Coarse Sand	Coarse Sand	Poorly Sorted	Strong Coarse Skewed	Coarse Sand	Coarse Sand	Well Sorted	Strong Coarse Skewed
M6	SE	Granule	Granule	Moderately sorted	Strong Coarse Skewed	Coarse Sand	Granule	Poorly Sorted	Strong Coarse Skewed	Very Coarse Sand	Very Coarse Sand	Poorly Sorted	Strong Coarse Skewed
M7	E	Medium Sand	Medium Sand	Poorly Sorted	Strong Fine Skewed	Coarse Sand	Coarse Sand	Moderately Well	Strong Coarse Skewed	Coarse Sand	Coarse Sand	Poorly Sorted	Strong Coarse Skewed
M8	E	Fine Sand	Fine Sand	Poorly Sorted	Strong Coarse Skewed	Granule	Granule	Poorly Sorted	Strong Coarse Skewed	Very Coarse Sand	Very Coarse Sand	Moderately Well	Fine Skewed
M9	NE	Very Coarse Sand	Very Coarse Sand	Moderately Well	Strong Fine Skewed	Coarse Sand	Coarse Sand	Well Sorted	Strongly fine skewed	Coarse Sand	Coarse Sand	Moderately Sorted	Strongly fine skewed
M10	NE	Very Coarse Sand	Very Coarse Sand	Poorly Sorted	Strong Coarse Skewed	Very Coarse Sand	Granule	Poorly Sorted	Strong Coarse Skewed	Very Coarse Sand	Very Coarse Sand	Moderately Well	Strongly fine skewed
M11	N	Medium Sand	Medium Sand	Moderately Sorted	Strong Coarse Skewed	Very Coarse Sand	Very Coarse Sand	Poorly Sorted	Strong Coarse Skewed	Coarse Sand	Coarse Sand	Moderately Well	Strongly fine skewed
M12	N	Coarse Sand	Coarse Sand	Poorly Sorted	Strong Fine Skewed	Very Coarse Sand	Very Coarse Sand	Poorly Sorted	Strong Coarse Skewed	Medium Sand	Medium Sand	Poorly Sorted	Strong Coarse Skewed
M13	NW	Coarse Sand	Coarse Sand	Moderately Well	Strong Fine Skewed	Coarse Sand	Coarse Sand	Well Sorted	Fine Skewed	Coarse Sand	Coarse Sand	Well Sorted	Strongly fine skewed
M14	NW	Coarse Sand	Coarse Sand	Well sorted	Strong Coarse Skewed	Coarse Sand	Coarse Sand	Mod. Well	Strongly fine skewed	Coarse Sand	Coarse Sand	Moderately Well	Strong Coarse Skewed
M15	W	Medium Sand	Medium Sand	Moderately Well	Strong Coarse Skewed	Coarse Sand	Coarse Sand	Well Sorted	Fine Skewed	Coarse Sand	Coarse Sand	Well Sorted	Strongly fine skewed
M16	W	Granule	Granule	Poorly Sorted	Strong Fine Skewed	Coarse Sand	Coarse Sand	Moderately Sorted	Strongly fine skewed	Very Coarse Sand	Very Coarse Sand	Well Sorted	Symmetrical

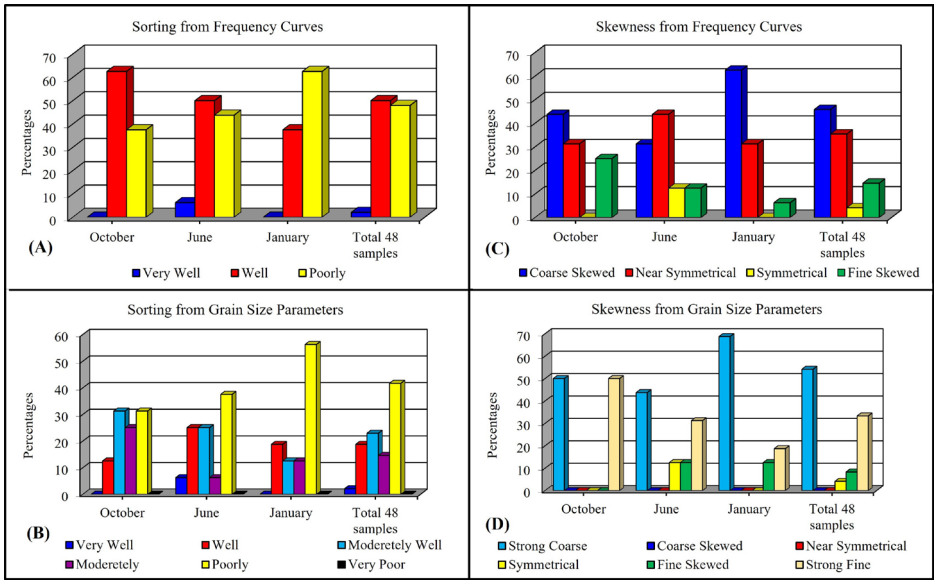

Fig. 7. Histograms showing percentage of sorting and Skewness from histograms compared to parameters equations.

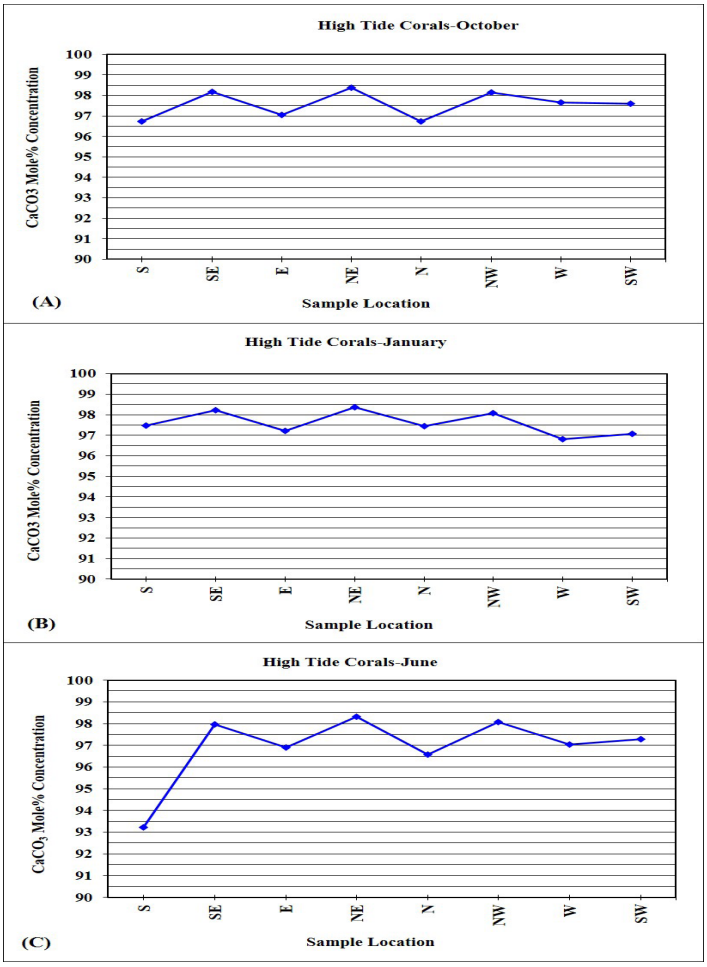

Fig. 8. Line graphs showing the distribution of CaCO3 Mole% concentration within coral fragments collected from the high tide mark around Umm Al-Maradim Island.

TABLE 6. List of Major and trace elements concentrations within coral fragments collected from high tide mark.

	No.	Sample Location	Mole %		Element ppm										
			$CaCO_3$	$MgCO_3$	Na	Al	Si	K	Fe	Sr	Pb	Zn	Cu	Co	Cr
October Coral Samples	1	S	96.74	3.26	6000	1080	4780	340	630	6740	BDL	BDL	0.893	0.446	0.645
	2	SE	98.16	1.84	3735	139		249	245	7459					
	3	E	97.05	2.95	8700	690	3510	550	620	6320	BDL	0.493	7.882	0.493	0.985
	4	NE	98.37	1.63	4935	206		217	343	6704					
	5	N	96.72	3.28	8640	2480	5310	470	430	6600	BDL	8.466	1.643	0.448	0.697
	6	NW	98.14	1.86	4313	214		334	379	7771					
	7	W	97.66	2.34	6140	1080	4550	290	620	6030	BDL	BDL	1.657	0.39	0.634
	8	SW	97.59	2.41	5720	1220	3860	370	520	5990	BDL	BDL	1.944	0.449	0.449
January Coral Samples	9	S	97.46	2.54	9990	1140	4090	640	440	6610	BDL	0.499	9.481	0.449	0.599
	10	SE	98.23	1.77	3180	243		272	386	7611					
	11	E	97.2	2.8	8150	1640	4350	500	410	6320	BDL	0.5	12	0.45	0.65
	12	NE	98.37	1.63	4020	199		147	352	6590					
	13	N	97.44	2.56	5310	2660	4550	340	520	6390	0.19	BDL	9.515	0.428	0.523
	14	NW	98.08	1.92	3623	265		343	359	7693					
	15	W	96.8	3.2	5080	930	4500	440	660	6420	BDL	BDL	1.992	0.498	0.747
	16	SW	97.07	2.93	9690	1030	4070	420	540	6520	BDL	BDL	2.815	0.477	0.716
June Coral Samples	17	S	93.23	6.77	16300	27300	13000	1040	1080	6500	BDL	BDL	0.849	0.45	0.5
	18	SE	97.96	2.04	3149	249		308	340	7578					
	19	E	96.9	3.1	9300	3180	4520	440	630	5890	0.436	0.339	4.845	1.938	1.938
	20	NE	98.32	1.68	4545	214		260	296	7066					
	21	N	96.58	3.42	8670	1400	4760	390	560	6870	BDL	BDL	0.446	0.446	0.842
	22	NW	98.07	1.93	4753	191		262	300	7863					
	23	W	97.02	2.98	5180	3380	4620	410	450	7010	BDL	BDL	6.018	0.44	0.587
	24	SW	97.28	2.72	8810	680	4300	410	530	7440	BDL	BDL	0.697	0.598	0.498

of Chromium, Cobalt and Cupper according to sample location (S, E, N, W, and SW only) and in the different seasons. Figure 10-B, D, and F are staked graphs showing the relationship between the concentration levels throughout the seasons. It clearly indicates that all the concentrations at the S, E, and N show a pathetic relationship, and the highest concentrations found at the eastern direction within all the seasons. Table 6 and Figure 10 show that the lowest trace element concentration levels is in corals gathered from the south direction during October, the western direction during January, and SW direction during June.

Discussion

The intertidal zone of Umm Al-Maradim Island is considered to be part of the back reef environment bordering the entire island. Coastal tides disperse reef debris along the island beaches. Normally back reef environments are affected by increased turbidity and decreased nutrients. Hence, these limitations result in the dominance of green algae, mollusks, grazers, foraminifera, and burrowers (Sellwood, 1991). The carbonate grains of modern sediments have different mineralogies and comprised of aragonite, and high-Mg and low-Mg calcite (Tucker and Wright, 1990; Tucker, et. al. 1990; Tucker, 2003). Brachiopods are mainly made of low-Mg calcite, bivalves (scallops, oysters, mussels, and serpulids skeletal) are bioclasts which initially made of low-Mg calcite, crinoids, bryozoans, calcareous red algae, rugose corals are bioclasts comprised of high-Mg calcite, and bioclasts such as many bivalves, gastropods, Scleractinia corals, green algae are originally composed of aragonite (Tucker and Wright, 1990). Calcite is normally classified as low magnesium calcite (Low-Mg calcite) with less than 4 Mole% $MgCO_3$, and high magnesium calcite (high-Mg calcite) with greater than 4 Mole% $MgCO_3$, but typically ranges between 11-19 Mole% $MgCO_3$ (Tucker, 1981; Tucker and Wright, 1990). Calcium carbonate is also found as Aragonite, which is orthorhombic, and normally with very low Mg content (< 5000 ppm), and high in strontium content (up to 10,000 ppm = 1% Sr) (Tucker, 1981; Tucker and Wright, 1990). Low-Mg calcite is commonly found in most of the seawater organisms such as bivalves, brachiopods, sponges, ostracods, pelagic foraminifera, and algae. While high-Mg calcite is commonly found in tabulate corals, sponges, echinoderms, ostracods, foraminifera, and algae. All recent mollusks are commonly composed of aragonite rather than calcite. Scleractinia corals (Triassic to Recent) have aragonitic skeletons.

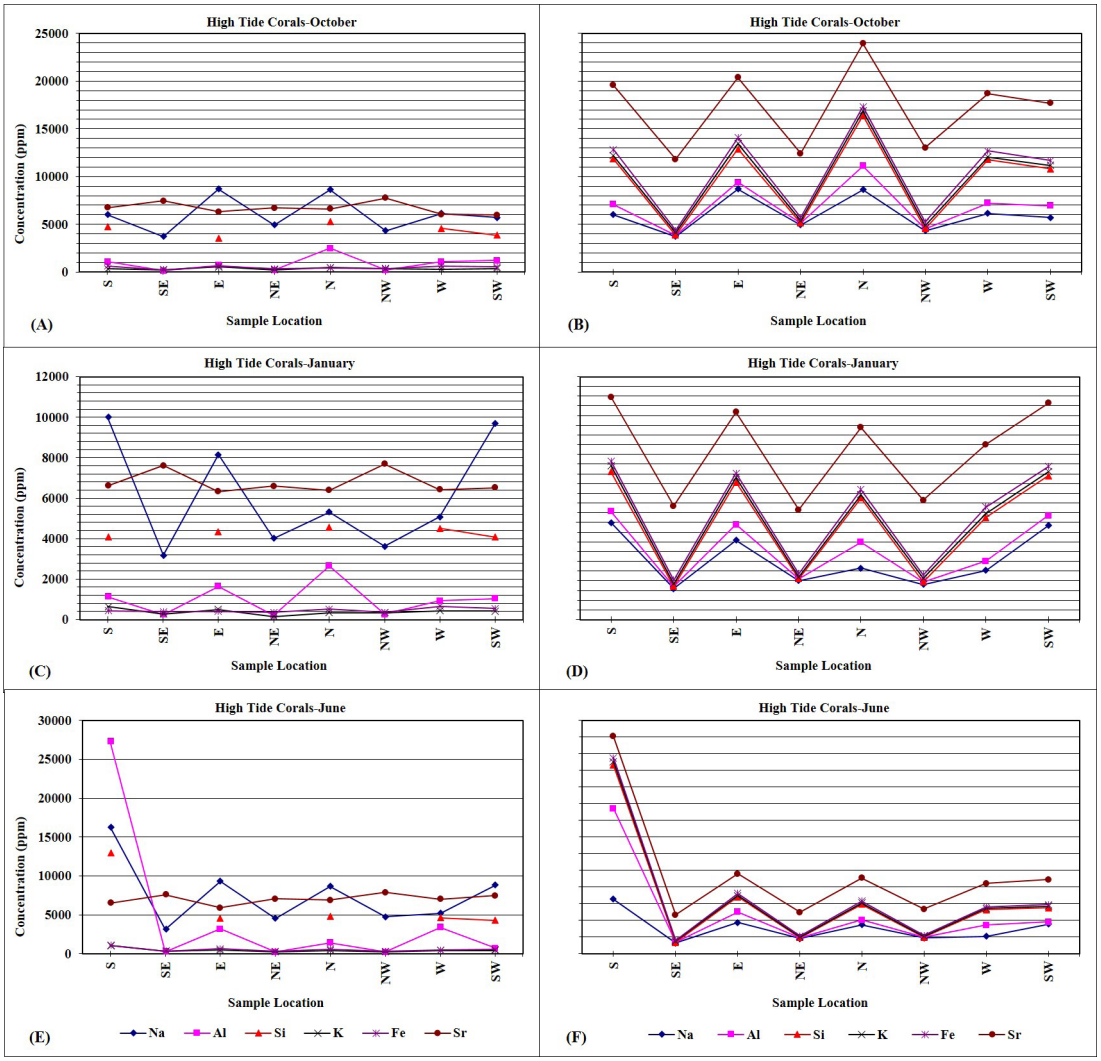

Fig. 9. Line graphs showing the distribution of major elements concentrations within coral fragments collected from the high tide mark around Umm Al-Maradim Island.

In the case of the present study $CaCO_3$ Mole% range between 93.23 to 98.37 Mole% and $MgCO_3$ range between 1.63 to 6.77 Mole% where the lowest $CaCO_3$ Mole% and highest $MgCO_3$ Mole% concentration levels found within corals collected during June, specially from the southern direction of the island. Mole % $MgCO_3$ indicate that there exist both low-Mg calcite and high-Mg calcite. The results of chemical study for strontium within all the collected coral fragments indicated that it ranges between 5890-7863 ppm, which implies that the low magnesium percentages coupled with high strontium indicate that coral fragments are of Aragonite rather than low-Mg calcite composition. When linking chemical data to weather parameters it appears that when winds are generally blowing from the south and southwest, after January up to June, corals will be more Mg-rich, hence composed of high-Mg calcite. Moreover, when wind is mainly blowing from the Northwest, before and up to October, and when wind will be calm and humidity high and temperature is moderate, after October up to January, corals will be Ca-rich, hence composed of aragonite and or low-Mg calcite. It appears that wind direction is the controlling factor for corals in either retaining their original aragonitic composition or being replaced by low-Mg calcite. The slight enrichment in magnesium in corals collected in June indicate cementing episode by high-Mg calcite crystals rather than diagenetic replacement of original coral composition. The cementation by high-Mg calcite is verified by the petrographic study, where it is more pronounce within sediments collected during June. Moreover, geochemical data indicate that all the highest concentrations levels for N, K, Al, Fe, Si, Cr, Co, and Cu are obtained from coral fragments

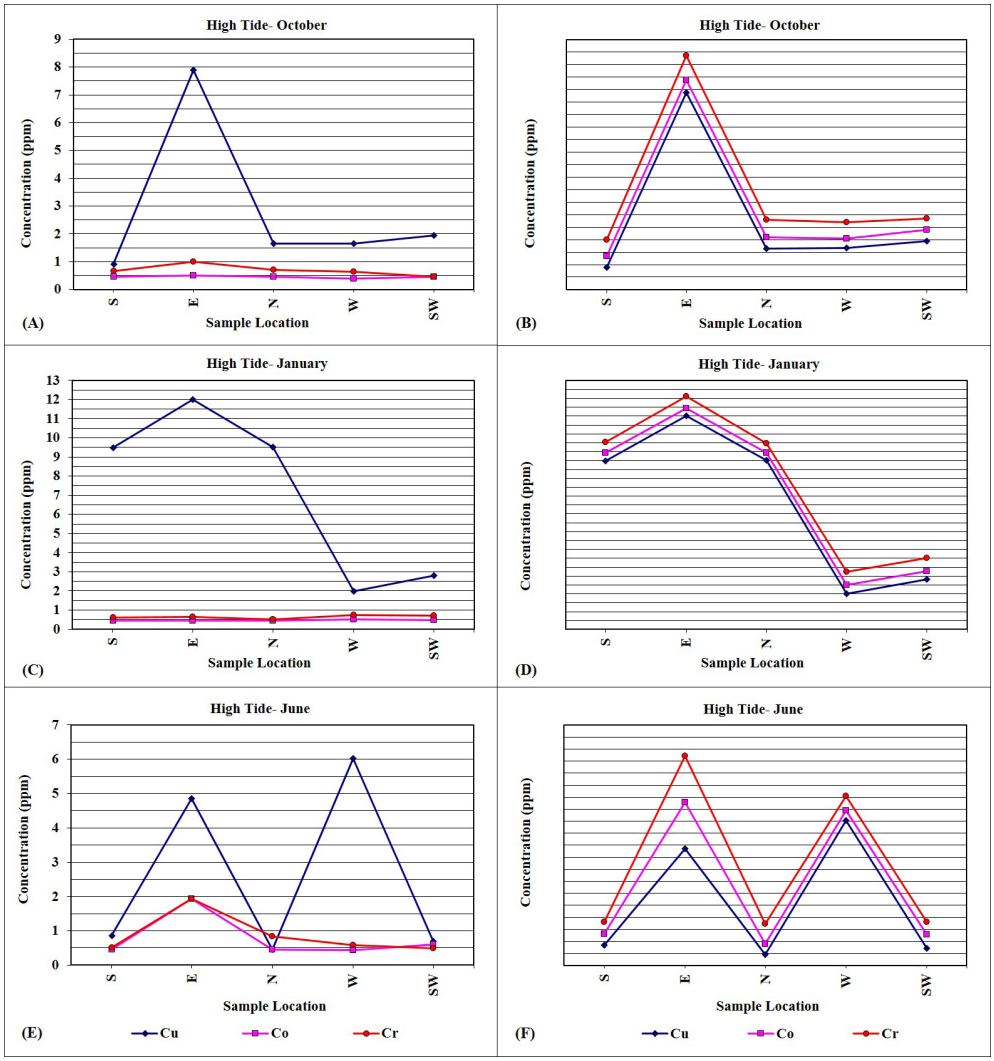

Fig. 10. Line graphs showing the distribution of trace elements concentrations within coral fragments collected from the high tide mark around Umm Al-Maradim Island.

collected from the south of the island during the month of June, except for Sr data the highest concentration is within coral fragments collected from the NW in June (Fig. 9 and 10). Therefore, when the coral composition is slightly Mg-rich it will have the highest concentration of all major elements.

The Petrographic study of all collected samples from the intertidal zone around Umm Al-Maradim Island showed that there is homogeneity in samples components, where all suggest a back-reef environment. Petrographic data revealed that sediments accumulated through January and June are of more various kinds than sediments accumulated throughout October. This is possibly an effect of wave action, temperature of marine water, and wind velocity around the island. Usually, there will be a decrease in temperature and increase in humidity during and after October, which result in shortage of nutrients and oxygen for the wellbeing of corals reefs. Hence the death of the corals during winter season. Additionally, coral grazers such as predatory types of fish and echinoderms will cause bioerosion of corals reefs and buildup of numerous varieties of coral fragments within the intertidal environment following October. Furthermore, during January water temperature considered to be the lowest, but tends to be moderate towards the end of February until March boosting the growth of algae. April and May represent the monsoon weather season in Kuwait which is characterized by increase in wind activity hence high wave action, and thunder rainstorms. These weather factors will cause the breakdown and production of various types of coral particles initially

through destroying coral polyps as a result to decreasing temperature levels, then by the effect of flourishing grazers such as echinoderms, algae, predatory type of fish, and endolithic bacteria. All these processes will ease the breakdown of the unstable reefs by means of high wave action. High quantities of echinoderms have been noticed dwelling during June and October within intertidal and subtidal environment around the island. Generally, echinoderms tend to feed on coral polyps leaving the coral buildups white and bare. This event is called coral bleaching and it has been recorded to be the main factor in the death of corals living in the Red Sea and Arabian-Percian Gulf (Wilson et. al. 2002; Goldberg and Wilkinson, 2004; Al-Horani et. al. 2011; Kteifan, 2017; Al-Horani et.al. 2021). Carballo et.al. (2013) indicated that boring sponges can cause bleaching of corals, where not only result in the destruction of coral life but also weakening the union of the colony and promoting their breaking down into smaller pieces. They also postulated that worldwide increasing temperature will rise sponge colonies that result in damaging coral mounds globally. As for the corals around Umm Al-Maradim Island, coral bleaching and disintegration may be the result of increase temperature during end of spring through summer and beginning of Autumn seasons (May-October) which induce the increase in coral grazers such as echinoderms and sponges. This event is very evident and was confirmed by the petrographic and grain size analysis of coral sediments.

Another factor enhancing the effect of coral bleaching and disintegration around Umm Al-Maradim Island is oil pollution. Most of the samples show the accumulation of oil particles within the intragranular porosity of the coral fragments. It has been recorded that oil contamination is one of the key factors in killing the coral communities, hence breakdown of coral reefs (Kteifan, 2017). Source of oil around Umm Al-Maradim Island is the oil tankers which pass through the marine territorial area near the island on their way to oil harbors along the coast of Kuwait. It is observed that these tankers used to discharge the water held in the tankers oil-reservoir into the sea before reaching the harbors. In addition, oil seepage is frequent from the area north of Umm Al-Maradim, especially around Qaruh Island, where marine currents can easily spread the oil spill south-wards.

Petrographic study revealed that even that all accumulated sediments are comprised of similar components, they differ on bases of diagenetic processes which prevailed after deposition along the back-reef environment. It is noted that aragonite and halite cement dominated throughout June and October. Additionally, detached Mg-calcite, aragonite, and halite crystals of sizes ≤ 0.032 mm are part of the sediments. An additional important difference is precipitation of microcrystalline yellowish-orange, yellowish-brown, and yellow carbonate mud, gypsum, and halite on particles. Although this precipitate is observed in all accumulated sediments throughout January, it is missing from accumulated deposits throughout June and October.

Generally, formation of hard ground starts with the lithification of the different particles on the seabed after deposition. Fibrous Mg-calcite and aragonite cements, coating grains and fossils and lining cavities forming botryoidal cements, is generally of marine origin and is common in reef-rocks, mud mounds and stromatolitic structures (Tucker and Bathurst, 1990; and Tucker, 2003). Tucker and Bathurst (1990) indicated that high Mg-calcite generally occurs as isopachous rinds, Mg-calcite micrite, and Mg-calcite spars, while aragonite never form isopachous rinds, but form either mesh of needle cement or botryoidal cements within cavities. Aragonite cements in reefs can form as 2 cm long euhedral pseudohexagonal crystals and later microcrystalline 'dendrites' locally almost occluding primary pores (Pichler and Dix, 1996; and Pichler and Veizer, 2004). It was indicated by Kleypas (1997), Malone (2001) and Montaggioni and Braithwaite (2009) that saturation state of ocean surface waters with respect to aragonite is temperature-dependent, and that in modern seas, sea surface temperature values and saturation state appear to be positively correlated. In a designed experiment to reproduce cementation of beach rocks by Neumeier (1999), marine conditions were simulated, such as tidal movements, evaporation rate, temperature, and water composition, and controlling the water salinity and saturation. Neumeier, 1999, found out that a variety of cements were generated including bladed and micritic high-magnesium calcite, and micritic and acicular aragonite. Jaramillo-Vogel, et. al. (2019) indicated that fibrous aragonite crust and/or botryoidal aragonite can develop on different marine deposits such as bioclast and oolitic grains in addition to coral reefs.

The third significant processes are particle burrowing and micritization which develop due to endolithic bacteria and flourishing algae on grains lying on the sea floor. These processes create micritic cover encircling the bioclasts, formation of pore spaces, and absence of luster due to eroded external surface of carbonate grains. It should be noted that burrowing and micritization of carbonate grains was considerable higher throughout January. It is attributed to reduction of wind velocity, thus calming of marine waters due to

decrease wave erosion, and to mild water temperature which enhances algal growth and booming.

Data from sieving technique indicated the influence of elevated wave activity around Umm Al-Maradim Island. This is related to Umm Al-Maradim Island geographic setting is the southernmost wide-open marine area of Kuwait. Thus, Umm Al-Maradim Island faces the northwestern winds, which cause elevated waves activity especially at the N, NW, and W sides. The direct effect of high wave activity throughout October is reflected on grain sizes of the accumulated sediments, where the data indicate that Median, Mean and Mode results equals to coarse sand size (0.5 – 1.0 mm). Whereas the majority of accumulated sediments prior to and throughout June show that the most common grain sizes are very coarse and coarse sand size (2-0.5 mm), which is directly related to the prevailing southeastern wind direction. Samples accumulated prior to and throughout January show that wave action and wind are intense, which is reflected on grain sizes of the accumulated sediments, where the data indicate that Median, Mean and Mode results equals to coarse sand size (0.5 – 1.0 mm).

Results of sieving technique showed that all accumulated sediments during June and October suggest that almost the entire high tide deposits are well to moderately sorted, whereas samples gathered from low tide mark are poorly sorted. As for samples gathered during January, nearly all samples from high tide and low tide marks are poorly sorted. All this data can be linked directly to the prevailing wind direction and speed, where in Kuwait normally summer and autumn months are affected by high velocity winds which can cause increase in wave action along the beaches causing better sorting in high tide sediments. Data also suggests that samples show a general decrease in sorting between October and January, where most of the samples are poorly sorted. It indicates that weather parameters which resulted in the primary breakup of primary coral reefs produced gravel size particles needed to be reworked for a very long period to produce finer particles as end member. Therefore, the poorly sorted nature of the back-reef deposits developed due to a short distance of transportation accompanied by relatively rapid accumulation of transported grains. Skewness results suggest that most of the accumulated sediments are strongly coarse skewed, both for overall sum of samples and samples in each season. In addition, accumulated deposits throughout January show the highest percentage of strongly coarse skewed results than Summer and Autumn seasons. Hence, skewness implies that wave activity all around Umm Al-Maradim Island is mostly high which leads to flushing out of fine fragments.

Conclusions

Grain size analysis showed that: 1) The majority of fragments composing the accumulated back-reef deposits around Umm Al-Maradim Island have sizes which is equal to coarse and very coarse sand size; 2) fine size particles are the least abundant; 3) Umm Al-Maradim Island is influenced by elevated wave and winds action especially throughout spring , summer and autumn seasons which resulted in the disintegration of coral reefs and result in to buildup of debris of various sizes around the island. Petrographic study indicated that grain composition is equivalent to a back-reef environment with a short distance of transport. The disintegration of coral particles is mainly due to wave action and coral bleaching effect by other organisms such as echinoderms and sponges. Grain micritization is higher during winter seasons due to calming of the sea and preferred temperature for the flourishing of endolithic bacterial and green algae. Additionally, the occurrence of aragonite, calcite, gypsum, and halite cement crystals and/or separate crystals is greater throughout June and October. Geochemical data support the retention of coral original composition of aragonite and low-Mg calcite, and the slight enrichment in Mg is due to the cementation of intragranular porosity by high-Mg calcite specially during spring and early summer (February-June).

All petrographic features, grain size analysis data, and chemical differences within sediments gathered from intertidal back-reef environment around Umm Al-Maradim Island signify close relationship with climate constraints and environmental controls, particularly wind speed and direction, water and air temperature, humidity, and salinity of marine waters.

Acknowledgments

The author is grateful to The Director General for the Public Authority for Applied Education and Training (PAAET) for supporting the usage of research equipments and financing (Research Grant No. BE 01 007). I express my thanks to the chief technicians at the university of Manchester-Earth and Environmental Science Department for chemical analyses of samples. There is no conflict of interest between the researcher and The University of Manchester. I would also like to give my special thanks to my colleague Dr. Ahmad Mohamed Morsy for his classification of foraminifera species.

References

Al-Ghadban, A. N. (1994) Morphology, sedimentology, and mineralogy of southern islands of Kuwait, Arabian Gulf. Journal of Kuwait Univ. of Sci., 21, 265-289.

Al-Ghadban, A. N., Abdul Rahman, M., and Salman, A. (1990) Physiographic and hydrographic features of Kubber, Qaruh and Umm Al-Maradim Islands. Kuwait Institute for Scientific Research, Report No: KISR 3419, Kuwait.

Al-Horani, F. A., Hamdi, M. & Al-Rousan, S. (2011) Study of Drupella cornusprey selection 270and grazing on corals from the Jordanian coast of the Gulf of Aqaba-Red Sea. Jordan Journal of Biological Sciences, 4 (4), 191-198.

Al-Horani, F., Al-Talafhah, S. T., kteifan, M., and Hussein, E. I. (2021) Stress response of the coral Stylophora pistillata towards possible anthropogenic impacts in the Gulf of Aqaba, Red Sea. Kuwait Journal of Science Accepted and fully citable articles not yet assigned to an issue. DOI: https://doi.org/10.48129/kjs.online

Al-langawi, A. J. (2013) The effect of climate on the chemical composition of the coral reefs around Kubber Island-Kuwait. International Journal of Geosciences, 4, 511-528. Doi: 10.4236/ijg.2013.42047

Carballo, J. L., Bautista, E., Nava, H., Cruz-Barraza, J. A., and Chavez, J. A. (2013) Boring sponges, an increasing threat for coral reefs affected by bleaching events. Ecology and Evolution, 3(4), 872–886 doi: 10.1002/ece3.452

Folk, R. L. (1974) Petrology of sedimentary rocks. Hemphills, Austin, Texas-USA, 159 p.

Folk, R. L., and Ward, W. C. (1957) Brazos River bar. A study in the significance of grain size parameters. Journal of Sedimentary Petrol., 27, 3-27.

Goldberg, J., and Wilkinson, C. (2004) Global threats to coral reefs : coral bleaching, climate change, disease, predator plagues, and invasive species. In : C. Wilkinson (Editor), Status of coral reefs of the world. Australian Institute of Earth Science, 1, 67-92.

Harrison, P. L., Alhazeem, S. H. and Alsaffar, A. H. (1997) The ecology of coral reefs in Kuwait and the effects of stressors on corals. Kuwait Institute for Scientific Research. Report No. KISR 4994, Kuwait, 43 p.

Jaramillo-Vogel, D., Foubert, A., Braga, J. C., Schaegis, J., Atnafu, B., Grobety, B., and Kidane, T. (2019) Pleistocene sea-floor fibrous crusts and spherulites in the Danakil Depression (Afar, Ethiopia). Sedimentology, 66, 480–512

Kassler, P. (1973) The structural and geomorphic evolution of the Persian Gulf. In: B. H. Purser (Ed.), The Persian Gulf. Springer-Verlag, Berlin, 11-32.

Kleypas, J. A. (1997) Modeled estimates of global reef habitat and carbonate production since the last glacial maximum. Paleoceanography, 12, 533–545.

Kteifan, M., Wahsha, D. M. and Al-Horani, F A. (2017) Assessing stress response of Stylophora pistillata towards oil and phosphate pollution in the Gulf of Aqaba, using molecular and biochemical markers. Chemistry and Ecology, 33(4), 281-294.

Malone, M. (2001) Early diagenesis of shallow-water preiplatform carbonate sediments, leeward margin, Great Bahama Bank (Ocean Drilling Program Leg 166). Geological Society of America Bulletin, 113 (7), 881-894.

Montaggioni, L. F. and Braithwaite, C. J. R. (2009) Quaternary Coral Reef Systems: History, Development Processes and Controlling Factors. First Edition, Elsevier, Oxford, United Kingdom, 532 p.

Neumeier, U. (1999) Experimental modelling of beachrock cementation under microbial influence. Sedimentary Geology, 126, 35–46.

Pichler, T., and Dix, G. R. (1996) Hydrothermal venting within a coral reef ecosystem, Ambitle Island, Papua New Guinea. Geology, 24, 435–438.

Pichler, T., and Veizer, J. (2004) The precipitation of aragonite from shallow-water hydrothermal fluids in a coral reef, Tutum Bay, Ambitle Island, Papua New Guinea. Chemical Geology, 207, 31-45.

Purser, B. H. (1973a) Sedimentation around bathymetric highs in the southern Persian Gulf. In: Purser, B. H (Editor), The Persian Gulf. Springer-Verlag, Berlin, 157-178.

Purser, B. H (Editor) (1973b) The Persian Gulf: Holocene carbonate sedimentation and diagenesis in a shallow epicontinental sea. Springer-Verlag, Berlin, 471 p.

Reading, H. G. (Ed.) (1991) Sedimentary environments and facies. Second edition. Blackwell Scientific Publications, Oxford, 615 p.

Sellwood, B. W. (1991) Shallow-marine carbonate environments. In: H. G. Reading, (Editor), Sedimentary environments and facies. Second edition. Blackwell Scientific Publications, Oxford, 283-342.

Sheppard, C. R. C. (1988) Similar trends, different causes: Responses of corals to stressed environment in Arabian Sea. Proceedings of the 6th International Coral Reef Symposium, Australia, 3, 297-302.

Tucker, M. E. (2003) Sedimentary Rocks in the Field. 3rd Edition. John Wiley & Sons Ltd, West Sussex, England. 237 p.

Tucker, M. E., and Bathurst, R. G. C. (Ed.) (1990) Carbonate Diagenesis. Reprint Series, International Association of Sedimentologist, Blackwell Scientific Publication, 1, 312 p.

Tucker, M. E., and Wright, V. P. (1990) Carbonate Sedimentology. Blackwell Scientific Publications, London, 482 p.

Tucker, M. E., Wright, V. P., and Dickson, J.A.D. (1990) Carbonate Sedimentology. Blackwell Science Ltd, a Blackwell Publishing company, 482 p.

Wilson, S., Fatemi, S. M. R., Shokri, M. R., and Claereboudt, M. (2002) Status of coral reefs in the Persian/Arabian Gulf and Arabian Sea region. In: C. R. Wilkinson (Editor), Status of coral reefs in the world. GCRMN Report, Australian Institute of Marine Science, chapter 3.

تأثير التغيرات المناخية الموسمية على الرواسب المتراكمة داخل بيئة الشعاب المرجانية الخلفية حول جزيرة أم المرادم - الكويت

إلهام جاسم اللنقاوي

الهيئة العامة للتعليم التطبيقي والتدريب، قسم العلوم، دولة الكويت

تعتمد هذه الدراسة على التحليل البتروغرافي والجيوكيميائي والميكانيكي لجميع العينات التي تم جمعها من المنطقة المحصورة بين أعلى مد وأدنى جزر حول جزيرة أم المرادم في جنوب الكويت. الهدف من هذه الدراسة هو تفسير تأثير الظروف المناخية المرتبطة بالمواسم المختلفة على تراكم الشعاب المرجانية حول الجزيرة. كشفت الدراسة البتروغرافية أن المنطقة المحصورة بين أعلى مد وأدنى جزر هي جزء من بيئة الشعاب المرجانية الخلفية التي تتكون من تراكم الحطام المرجاني المكسور، والطحالب المرجانية، والمثقبات، وجزيئات شوكيات الجلد، والرخويات ذوات الصدفتين، والرخويات بطنيات الأرجل. بشكل عام، تكون أحجام الرواسب الأكثر وفرة على طول الشواطئ ذات حجم رملي خشن ورملي خشن جدًا، مما يشير إلى مسافة قصيرة من النقل وحركة الأمواج العالية. أدت مسافة النقل القصيرة والترسيب السريع إلى تراكم رواسب سيئة الفرز وذات حيود خشن شديد إلى رواسب ذات حيود خشن. تظهر الدراسة التفصيلية للعينات اختلافات في معايير حجم الرواسب وكذلك نوع الرواسب المتراكمة بين الفصول والمواقع المختلفة على طول الجزيرة، والتي ترتبط بشكل أساسي بالاختلافات في شدة الرياح، والتغيرات في اتجاه الرياح السائدة ، والأنشطة البيولوجية التي تؤثر على الشعاب المرجانية. تشير الدراسة الجيوكيميائية إلى تكوين أراغونيتي وكالسيت منخفض المغنيسيوم ضمن بقايا المرجان المتراكم، بالإضافة إلى علاقة متساوية متناسقة بين كل العناصر التي تم تحليلها ضمن الرواسب التي تم جمعها من المنطقة المدية.